JOM, Vol. 70, No. 10, 2018
https://doi.org/10.1007/s11837-018-2972-3

Understanding the Strengthening Effect of β_1 Precipitates in Mg-Nd Using In Situ Synchrotron X-ray Diffraction

BIJIN ZHOU,[1] LEYUN WANG,[1,4] GAOMING ZHU,[1] JIE WANG,[1] WEN WEN,[2] and XIAOQIN ZENG[1,3,5]

1.—National Engineering Research Center of Light Alloy Net Forming, Shanghai Jiao Tong University, Shanghai 200240, China. 2.—Shanghai Institute of Applied Physics, Chinese Academy of Sciences, Shanghai 201204, China. 3.—State Key Laboratory of Metal Matrix Composites, Shanghai Jiao Tong University, Shanghai 200240, China. 4.—e-mail: leyunwang@sjtu.edu.cn. 5.—e-mail: xqzeng@sjtu.edu.cn

In situ synchrotron x-ray diffraction was carried out at beamline BL14B1 of Shanghai Synchrotron Radiation Facility (SSRF) to study the tensile deformation of an extruded Mg-2.2 wt.%Nd alloy before and after aging. The aged specimen that contained β_1 (Mg_3Nd) precipitates showed higher strength than the nonaged specimen, while the strain to failure of the two specimens was almost equal. Analysis of the lattice strain evolution in the aged specimen revealed a modest load-transfer effect from Mg to β_1 after 2% strain. Peak width analysis indicated that a high level of microstrain developed in β_1 immediately after material yielding. Ex situ transmission electron microscopy (TEM) showed strong interaction between basal dislocations and β_1 precipitates. Based on these results, it is proposed that the extra strength in the aged specimen is caused by β_1 impeding dislocation movement and eventually being sheared by dislocations.

INTRODUCTION

Mg and its alloys are promising structural materials for weight reduction in automotive and aerospace industries due to their low density and high specific strength.[1–3] However, the relatively low absolute strength of Mg alloys remains an obstacle to wider application of these materials.[4,5] Age hardening provides a useful approach to enhance the material strength, especially when the alloy contains rare-earth elements.[6,7] Nd is an effective alloying element that offers strong potential for age hardening of Mg alloys.[8–11] The precipitation sequence in Mg-Nd binary alloys has been studied extensively in recent years using both experimental and computational tools.[12–16] Among the various types of precipitates that have been observed under different aging conditions, β_1 [Mg_3Nd, face-centered cubic (FCC) structure, a = 7.4 Å] is recognized as a main strengthener, often being observed around peak aging conditions.[15] However, the actual strengthening mechanism has not been clarified so far, due to lack of in situ experimental data.

Recently developed synchrotron x-ray diffraction techniques provide a unique opportunity to study precipitate strengthening dynamically in various metallic materials.[17–23] Kada et al.[20] studied the deformation behavior of aged and nonaged AZ91 (Mg-9Al-1Zn, wt.%) alloys (i.e., with or without $Mg_{17}Al_{12}$ precipitates). Based on lattice strain analysis, it was found that the $Mg_{17}Al_{12}$ precipitates in the aged alloy increase the critical resolved shear stress (CRSS) for basal slip by 5 MPa compared with values for the nonaged alloy. Garcés et al.[22] studied the compressive behavior of an extruded Mg-Y-Zn alloy that contained the long-period stacking order phase (LPSO). While deformation in the Mg matrix occurred early and was dominated by basal slip and twinning, the LPSO phase remained elastic, indicating typical load-transfer behavior from the soft Mg matrix to hard LPSO phase. Lentz et al.[23] studied the deformation behavior of an extruded Mg-Y-Nd alloy (WE54) in different aged conditions using electron backscattered diffraction (EBSD), in situ energy-dispersive synchrotron x-ray diffraction, and elastoplastic self-consistent (EPSC) modeling. It was found that {10-12} tension

(Published online June 11, 2018)

twinning activity increased significantly after age hardening at 250°C for 500 h when prismatic plate-shaped precipitate (β) became abundant in the Mg matrix. Simulation of the lattice strain evolution of the Mg phase by EPSC suggested that those β precipitates harden basal <a> slip more than other slip modes. On the contrary, the CRSS for twinning decreased after age hardening due to the reduced solute concentration of Y and Nd that form β precipitates.

In the present work, tensile deformation of an extruded Mg-2.2 wt.%Nd alloy with and without aging treatment was studied by in situ synchrotron x-ray diffraction. The higher strength of the aged specimen was attributed to β_1 precipitates formed during aging. Lattice strain analysis indicated that β_1 precipitates did not show the load-transfer effect at the beginning of plastic deformation, as found in many other precipitate-strengthened materials. A modest load-transfer effect was found after about 2% macroscopic strain. Peak broadening analysis indicated that β_1 precipitates accumulated a high level of microstrain upon material yielding. Combining these observations with ex situ transmission electron microscopy (TEM), the strengthening mechanism of β_1 precipitates is elucidated.

MATERIALS AND METHODS

An as-cast Mg-2.2 wt.%Nd cylindrical billet with diameter of 58 mm was treated by solid solution (T4) at 540°C for 24 h, followed by water quenching. After that, the billet was extruded at 500°C with reduction ratio of 18:1 and subsequently annealed at 530°C for 15 min. Sheet specimens for tensile tests with nominal gauge dimensions of 17 mm × 1.4 mm × 1.0 mm were prepared by electron discharge machining, with tensile axis parallel to the extrusion direction (ED). Specimens in this condition are named "annealed." "Annealed" specimens showed a single Mg phase with average grain size of ~ 70 μm according to EBSD characterization. Half of these "annealed" specimens were subsequently aged at 240°C for 5 h to allow β_1 precipitates to form in the material ("aged"). Figure 1a shows a bright-field TEM image (JEOL, JEM 2100F) of an "aged" specimen viewed along $[0001]_{Mg}$ direction, where β_1 precipitates with platelet shape are distributed homogeneously in the Mg matrix. β_1 precipitates have the following orientation relationship with the Mg matrix: $(110)_{\beta1}//(0001)_{Mg}$ and $(-112)_{\beta1}//(1-100)_{Mg}$.[11,12]

In situ tensile tests using an annealed specimen and an aged specimen were conducted at beamline BL14B1 of Shanghai Synchrotron Radiation Facility (SSRF).[24] Each specimen was loaded using a commercial testing module (MTI, SEMtester 1000 lb) at constant tensile speed of 0.2 mm/min (corresponding to initial strain rate of 2.0×10^{-4} s^{-1}). During loading, the gauge center of the specimen was illuminated by a transmissive

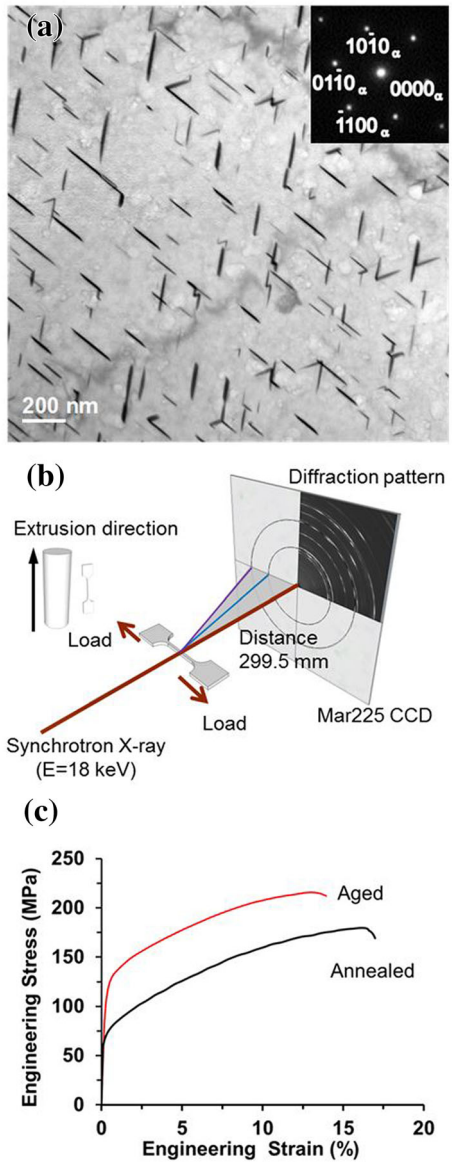

Fig. 1. (a) Bright-field TEM image of an "aged" specimen. (b) Schematic of in situ tensile experiment with synchrotron x-ray diffraction. (c) Stress–strain curves of aged and annealed specimens from in situ experiment.

x-ray beam (beam size = 200 μm × 200 μm) with energy of 18 keV (λ = 0.6884 Å). A Mar225 x-ray detector with an array of 3072 × 3072 pixels continuously recorded two-dimensional (2D) diffraction patterns from the specimen every 5 s during the entire tensile test until fracture. The exposure time for acquiring each diffraction pattern was 0.5 s. According to the calibration using standard LaB_6 powder, the specimen-to-detector distance was approximately 299.4 mm. Figure 1b and c show the experimental setup and the tensile stress–strain curves of the annealed and aged specimens. The yield strength ($\sigma_{0.2}$) of the aged specimen (87 MPa) was apparently higher than that of the annealed specimen (64 MPa), which is attributed to the

existence of β_1 precipitates in the former material. Interestingly, the two specimens showed similar strain to failure. This is in contrast to some other precipitate-strengthened Mg alloys, where the material ductility is significantly compromised after aging treatment.[25,26] The effect of β_1 precipitates on the mechanical properties of the material is investigated below using in situ synchrotron x-ray diffraction data.

RESULTS

Figure 2a–c shows a series of 2D diffraction patterns obtained from the aged specimen at three different strains: 0, 2.3, and 12.5%. At 0% strain, the diffraction pattern shows discrete diffraction spots as a result of the large grain size. Given the Mg grain size of about 70 μm, it is estimated that the illuminated volume (200 μm × 200 μm × 1 mm) contains about 130 grains. After deformation, the diffraction rings gradually elongated along the azimuthal direction due to dislocation activity. To study the lattice strain evolution, diffraction profiles of intensity versus 2θ were obtained by integrating the 2D diffraction patterns over the azimuthal angle range of $-5°$ to $+5°$ around the axial direction using Fit2D software.[27] Diffraction peaks from both the Mg phase and β_1 phase could be indexed,[15] as shown in Fig. 2d. As the strain was increased, both peak shifting and broadening occurred. From the peak shift, the lattice strain can be measured as

$$\varepsilon_{hkl} = (d_{\sigma,hkl} - d_{0,hkl})/d_{0,hkl}, \quad (1)$$

where $d_{0,hkl}$ and $d_{\sigma,hkl}$ represent the d-spacing of the $\{hkl\}$ plane (calculated from the 2θ value) before deformation and under load, respectively.[19,22]

Figure 3 shows the lattice strain evolution of Mg and β_1 with the engineering strain (ε). In the elastic regime ($\varepsilon < 0.2\%$), the four Mg grain families and the three β_1 grain families show similar linear increase of their lattice strain value. Mg (0002) yielded first, followed by Mg (10-11), Mg (10-12), and finally Mg (10-10). Since the Mg (0002) grain family has near-zero Schmid factor for basal and other <a> slip modes, its early yielding must be attributed to twinning. The Mg (10-11) and Mg (10-12) grain families have their basal planes inclined nearly 45° to the tensile axis, making basal <a> slip easy to activate. The Mg (10-10) grain family would have to resort to prismatic slip to accommodate its deformation. The observation that Mg (0002) showed no hardening while the other three Mg grain families showed strong hardening suggests that β_1 precipitates inhibit dislocation propagation more than twin growth. This is consistent with the result in Ref. [23]. Lattice strain in β_1 showed a steady increase with strain. At first, the lattice strain increase in β_1 was close to that in Mg (10-11) and Mg (10-10), and even lower than that in Mg (10-10). When the engineering strain reached 2%, the lattice strain in β_1 eventually surpassed that in Mg, showing a modest load-transfer effect in later deformation. This observation is different from precipitate-strengthened steels, where carbide precipitate phases often develop much higher lattice strain than the Fe phase instantly upon yielding.[17,19]

To understand the strengthening mechanism by β_1, a TEM bright-field image was taken for an aged specimen after 0.5% strain (Fig. 4). The electron beam was along the $[2\text{-}1\text{-}10]_{Mg}$ direction. β_1 precipitates are parallel to the (0-110) prismatic plane. In addition to β_1 precipitates, lines with dark contrast are observed. These lines are identified as basal <a> dislocations that are parallel to the (0002) basal plane. Note that many of these dislocations were confined between β_1 precipitates. This observation suggests that dislocations in the aged specimen had reduced mean free path due to the existence of β_1 precipitates. Those dislocations can only move when the external stress is high enough to allow them to bypass or shear across β_1. This process enhances the strength of the material, as discussed below.

DISCUSSION

The β_1 phase in Mg-Nd alloys is widely recognized as a strengthener for the material by impeding dislocation movement. To further assess this effect, diffraction peak width information is utilized. The full-width at half-maximum (FWHM) value of each peak was calculated from the diffraction profile at different strains using Origin™ software. Figure 5a and b compares the evolution of the FWHM of selected Mg and β_1 peaks with strain in the aged specimen and the annealed specimen. The FWHM of diffraction peaks is positively correlated with the microstrain in the phase. For Mg, this microstrain is mostly due to accumulation of dislocations. In both the aged specimen and annealed specimen, the FWHM of Mg peaks gradually increased with strain, suggesting an increase of the dislocation density. The FWHM values of Mg peaks in the aged specimen were slightly higher than those in the annealed specimen. A possible explanation is that the β_1–Mg interface facilitated nucleation of dislocations during deformation. As shown in Fig. 5a, the FWHM values of β_1 peaks were notably much higher than for Mg peaks. This indicates very high microstrain in those β_1 precipitates. In a very recent work, Bhattacharyya et al.[28] found that basal dislocations can actually shear across β' precipitates in WE43 (Mg-Y-Nd) alloys. Dislocation shearing across β' precipitates was also observed in Mg-Y.[29] β' precipitates in WE43 have platelet shape on {11-20} planes and also provide resistance against movement of basal dislocations. Given the similarity between β' precipitates in WE43 and β_1 precipitates in Mg-Nd, it is reasonable to assume that β_1 precipitates are also shearable by basal dislocations. High microstrain in β_1 is expected when it has been

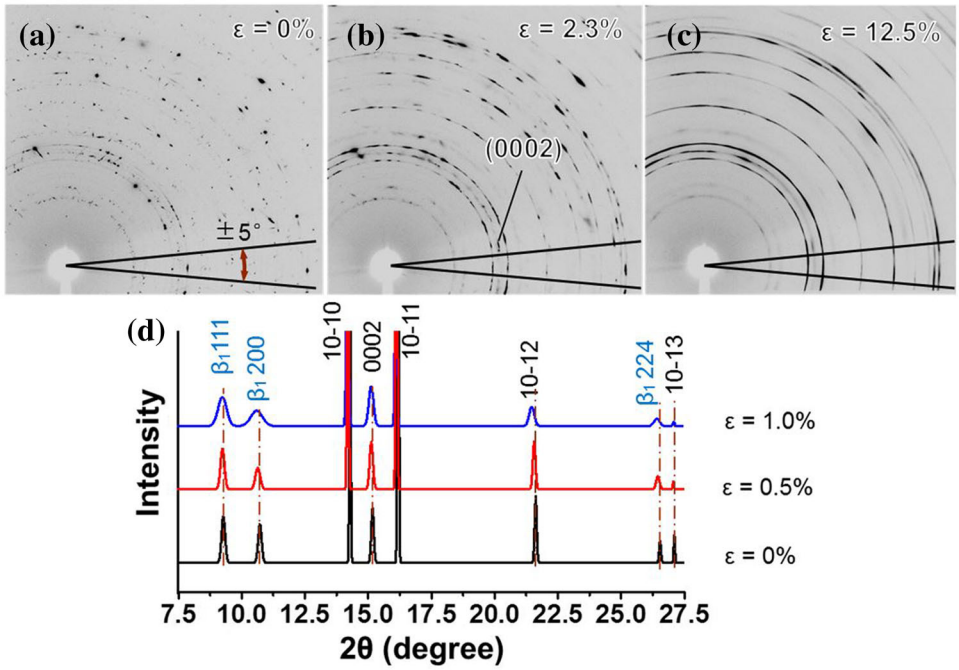

Fig. 2. (a–c) Diffraction patterns of the aged specimen at different strains. The area within the azimuthal angle range of − 5° to + 5° was integrated to study the lattice strain in Mg and β_1 phases. (d) Integrated diffraction profiles at three different strains. Peaks from Mg and β_1 are both indexed.

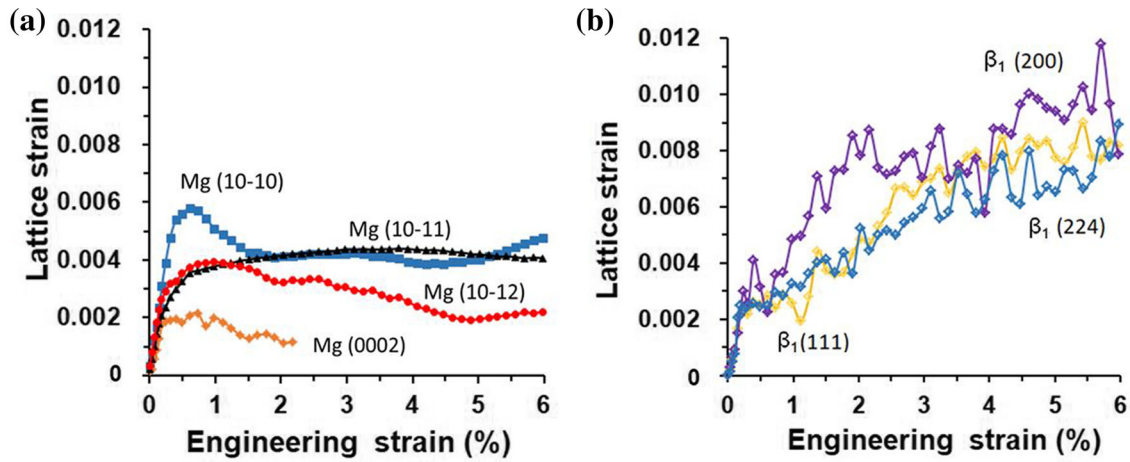

Fig. 3. Lattice strain evolution with the engineering strain for (a) Mg peaks and (b) β_1 peaks in the aged specimen.

sheared by dislocations. The result in Fig. 5a supports the argument that β_1 precipitates are more likely to be sheared than be bypassed by dislocations. When the volume fraction of β_1 is given, finer precipitates will minimize the mean free path of dislocations. This explains our previous finding that the peak strength of Mg-Nd alloys corresponds to the aging condition when a large volume of fine β_1 precipitates have been generated from the Mg matrix.[15]

This work shows that in situ synchrotron x-ray diffraction is a powerful tool to study the deformation behavior of Mg alloys with precipitates. Compared with neutron diffraction, which is also often used,[30,31] synchrotron x-ray diffraction provides higher diffraction intensity, so in situ testing can be conducted much faster. More importantly, synchrotron x-ray analysis allows one to see the weak diffraction peaks of precipitates and perform lattice strain and peak broadening analysis to better

understand the strengthening mechanism by precipitate phases, as shown in this work. Results from such studies are useful for integrated computational materials engineering (ICME) of Mg, which requires reliable plasticity models that can describe the microstructure–property relationship. So far, most models have simulated the precipitate strengthening effect by increasing the CRSS values of various deformation modes.[23,28,31] It would be interesting to develop models that can simulate the lattice strain and peak broadening behavior of precipitates.

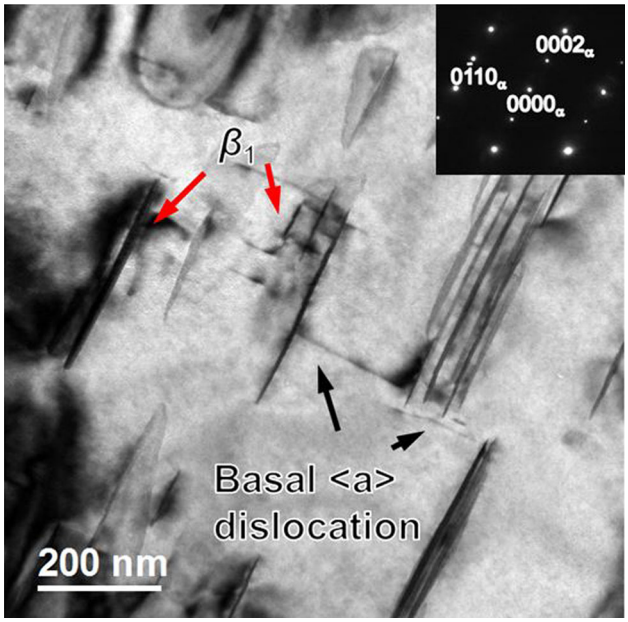

Fig. 4. Bright-field TEM image showing the interaction between β_1 precipitates and dislocations. The electron beam is along $[2\text{-}1\text{-}10]_{Mg}$ direction.

CONCLUSION

The deformation behavior of a Mg-2.2 wt.%Nd alloy before and after aging was compared. The aged specimen that contained β_1 precipitates showed higher strength than the annealed specimen, without sacrificing too much ductility. From in situ synchrotron x-ray diffraction data, the lattice strain in the β_1 phase was initially close to that of the hard grains in the Mg phase. After 2% macroscopic strain, the lattice strain in β_1 eventually surpassed that in Mg, indicating a modest load-transfer effect. According to peak broadening analysis, a high level of microstrain developed in β_1 immediately after material yielding. This was likely caused by β_1 impeding dislocation movement and eventually being sheared by dislocations. This is supported by ex situ TEM observation. Compared with dislocation movement, twinning is less inhibited by β_1.

ACKNOWLEDGEMENTS

This work is financially supported by the National Key Research and Development Program of China (No. 2016YFB0701203) and the National Natural Science Foundation of China (Nos. 51631006 and 51671127). L.W. is also sponsored by Shanghai Pujiang Program (No. 16PJ1404600). The authors thank beamline BL14B1 (Shanghai Synchrotron Radiation Facility) for providing beam time and help during experiments.

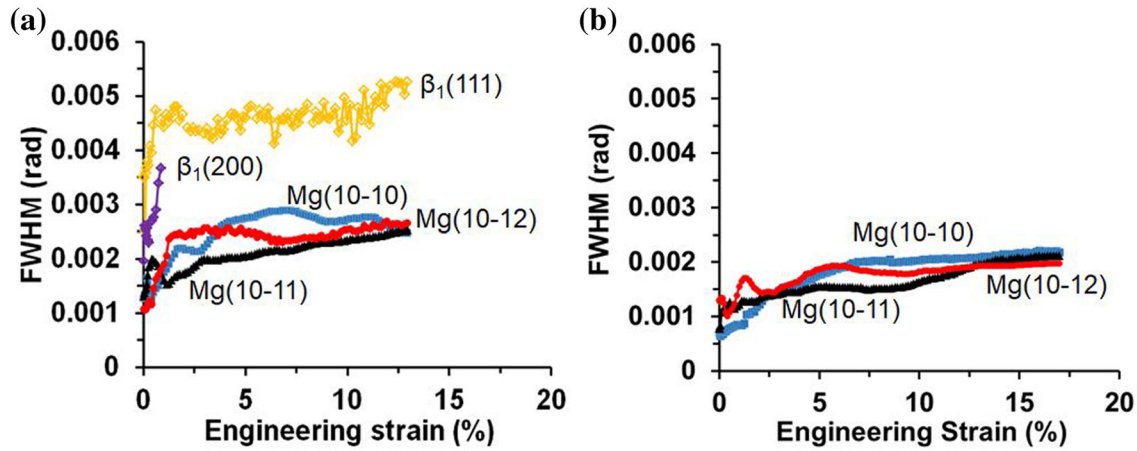

Fig. 5. Evolution of FWHM of selected Mg and β_1 peaks with strain in the (a) aged and (b) annealed specimen.

REFERENCES

1. A.A. Luo, *JOM* 54, 42 (2002).
2. A.A. Luo, *J. Magnes. Alloys* 1, 2 (2013).
3. B.C. Suh, M.S. Shim, K.S. Shin, and N.J. Kim, *Scr. Mater.* 30, 1 (2014).
4. T. Homma, N. Kunito, and S. Kamado, *Scr. Mater.* 61, 644 (2009).
5. K. Hono, C.L. Mendis, T.T. Sasaki, and K. Oh-ishi, *Scr. Mater.* 63, 710 (2010).
6. Z.J. Yu, Y.D. Huang, X. Qiu, G.F. Wang, F.Z. Meng, N. Hort, and J. Meng, *Mater. Sci. Eng. A* 622, 121 (2015).
7. X.Y. Xia, W.H. Sun, A.A. Luo, and D.S. Stone, *Acta Mater.* 111, 335 (2016).
8. A. Sanaty-Zadeh, A.A. Luo, and D.S. Stone, *Acta Mater.* 94, 294 (2015).
9. Y.Z. Ji, A. Issa, T.W. Heo, J.E. Saal, C. Wolverton, and L.Q. Chen, *Acta Mater.* 76, 259 (2014).
10. A. Issa, J.E. Saal, and C. Wolverton, *Acta Mater.* 65, 240 (2014).
11. K. Saito and K. Hiraga, *Mater. Trans.* 52, 1860 (2011).
12. J.F. Nie, *Metall. Mater. Trans. A* 43, 3891 (2012).
13. E.L.S. Solomon, V. Araullo-Peters, J.E. Allison, and E.A. Marquis, *Scr. Mater.* 128, 14 (2017).
14. S. DeWitt, E.L.S. Solomon, A.R. Natarajan, V. Araullo-Peters, S. Rudraraju, L.K. Aagesen, B. Puchala, E.A. Marquis, A. Van Der Ven, K. Thornton, and J.E. Allison, *Acta Mater.* 136, 378 (2017).
15. B. Zhou, L. Wang, B. Chen, Y. Jia, W. Wen, D. Li, D. Shua, P. Jin, X. Zeng, and W. Ding, *Mater. Sci. Eng. A* 708, 319 (2017).
16. D. Choudhuri, R. Banerjee, and S.G. Srinivasan, *Sci. Rep.* 7, 40540 (2017).
17. M.L. Young, J.D. Almer, M.R. Daymond, D.R. Haeffner, and D.C. Dunand, *Acta Mater.* 55, 1999 (2007).
18. G. Garcés, E. Oñorbe, P. Pérez, M. Klaus, C. Genzel, and P. Adeva, *Mater. Sci. Eng. A* 533, 119 (2012).
19. L.Y. Wang, M.M. Li, and J. Almer, *Acta Mater.* 62, 239 (2014).
20. S.R. Kada, P.A. Lynch, J.A. Kimpton, and M.R. Barnett, *Acta Mater.* 119, 145 (2016).
21. X. Zhang, M.M. Li, J.S. Park, P. Kenesei, J. Almer, C. Xu, and J.F. Stubbins, *Acta Mater.* 126, 67 (2017).
22. G. Garcés, D.G. Morris, M.A. Muñoz-Morris, P. Perez, D. Tolnai, C. Mendis, A. Stark, H.K. Lim, S. Kim, N. Shelld, and P. Adeva, *Acta Mater.* 94, 78 (2015).
23. M. Lentz, M. Klaus, M. Wagner, C. Fahrenson, I.J. Beyerlein, M. Zecevic, W. Reimers, and M. Knezevic, *Mater. Sci. Eng. A* 628, 396 (2015).
24. T.Y. Yang, W. Wen, G.Z. Yin, X.L. Li, M. Gao, Y.L. Gu, and L. Li, *Nucl. Sci. Technol.* 26, 1 (2015).
25. T. Honma, T. Ohkubo, S. Kamado, and K. Hono, *Acta Mater.* 55, 4137 (2007).
26. K.Y. Zheng, J. Dong, X.Q. Zeng, and W.J. Ding, *Mater. Sci. Eng. A* 489, 44 (2008).
27. http://www.esrf.eu/computing/scientific/FIT2D/.
28. J.J. Bhattacharyya, F. Wang, N. Stanford, and S.R. Agnew, *Acta Mater.* 146, 55 (2018).
29. E.L.S. Solomon and E.A. Marquis, *Mater. Lett.* 216, 67 (2018).
30. M.A. Gharghouri, G.C. Weatherly, J.D. Embury, and J. Root, *Philos. Mag. A* 79, 1671 (1999).
31. S.R. Agnew, R.P. Mulay, F.J. Polesak III, C.A. Calhoun, J.J. Bhattacharyya, and B. Clausen, *Acta Mater.* 61, 3769 (2013).